

# Use of $^{18}\text{F}$ -fluorodeoxyglucose positron emission tomography for diagnosis of uterine sarcomas

AKIRA NAGAMATSU<sup>1,2</sup>, NAOHIKO UMESAKI<sup>1,3</sup>, LI LI<sup>1</sup> and TETSUJI TANAKA<sup>1</sup>

<sup>1</sup>Department of Obstetrics and Gynecology, Wakayama Medical University, 811-1 Kimiidera,

Wakayama 641-8509; <sup>2</sup>Nagamatsu Ladies' Clinic, 628-1 Tottori, Hannan, Osaka 599-0204;

<sup>3</sup>Izumi Municipal Hospital, 4-1-10, Fuchu-cho, Izumi City, Osaka 541-0048, Japan

Received October 22, 2009; Accepted January 8, 2010

DOI: 10.3892/or\_00000734

**Abstract.** We evaluated the use of  $^{18}\text{F}$ -fluorodeoxyglucose positron emission tomography (FDG-PET) for the diagnosis of uterine sarcomas. FDG-PET combined with serum lactate dehydrogenase (LDH) levels were compared with FDG-PET alone for the diagnosis of leiomyosarcomas (LMS), which are the most difficult uterine sarcomas to diagnose. FDG-PET imaging of endometrial cancer (EC) was used as a reference. Immunoreactivity for glucose transporter-1 (GLUT-1) correlated with FDG uptake was evaluated in sarcomas and leiomyomas (LM), including cases not examined by FDG-PET. FDG was injected after at least 5 h fasting and standardized uptake values (SUVs) were analyzed quantitatively 50-70 min after injection. Immunohistochemical expression of GLUT-1 was studied in paraffin sections of tumors using anti-GLUT-1 antibodies and GLUT-1 expression scores were derived based on staining intensities. FDG-PET was performed preoperatively in a total of 53 patients including 10 with sarcomas, 19 with EC and 24 with LM. Immunohistochemical examination was performed in 17 sarcomas, 6 EC and 9 LM [6 usual LM, 1 uterine smooth muscle tumor of uncertain malignant potential (UMP), and 2 bizarre LM (BLM)]. SUVs for uterine sarcomas and EC were significantly higher ( $p=0.0001$ ) than those for LMs. There were no significant differences in SUVs among ECs, carcinosarcomas (CS) and LMS. Significant differences in SUVs existed between LM and LMS ( $p=0.003$ ). However, the diagnostic accuracy for LMS was only 73%. The diagnostic accuracy of FDG-PET combined with serum LDH was 100%. GLUT-1 expression scores were significantly higher in sarcomas and EC than in LM ( $p<0.0001$ ). Intermediate GLUT-1 scores were found in two of the three cases of UMP and BLM. In conclusion, FDG-PET is useful for diagnosing

uterine sarcomas, while FDG-PET combined with serum LDH is useful for diagnosing LMS. Immunohistochemical examination of GLUT-1 confirmed the high FDG uptake in LMS patients.

## Introduction

Uterine sarcomas mainly consist of leiomyosarcomas (LMS), carcinosarcomas (CS) and endometrial stromal sarcomas (ESS). These diseases are rare, with reported frequencies of 4-5% among uterine body malignancies. However, their prognoses are very poor, and an accurate diagnosis is therefore important. CSs are composed of carcinomatous and sarcomatous components. The former, though not the latter, can be detected by Pap smear tests. However, diagnosis of malignancy is very difficult in cases of LMS and ESS.

Current management of uterine leiomyoma (LM) often involves conservative therapy, e.g., with gonadotropin-releasing hormone (GnRH) agonists (1) or uterine arterial embolization therapy (2). The differential diagnosis of LM and LMS is therefore very important. Magnetic resonance imaging (MRI) has proven to be one of the most useful imaging modalities, but it is difficult to distinguish between LMS and LM with degeneration, even using MRI (3). The use of serum lactate dehydrogenase (LDH) levels for the diagnosis of LMS has also been reported (4,5), though the value of this technique for LMS diagnosis is limited by the fact that LDH levels are elevated in many different conditions.

$^{18}\text{F}$ -fluorodeoxyglucose positron emission tomography (FDG-PET) was recently introduced as a diagnostic technique for malignancies. FDG-PET provides functional imaging of malignant cells. It has been shown to be superior to MRI and/or computed tomography (CT) for evaluation of various malignancies (6). We have already reported on the usefulness of FDG-PET for the diagnosis of uterine sarcomas (7-9). However, several studies (10,11) have shown positive results for FDG-PET in cases of LM, and its usefulness in the differential diagnosis of LM and LMS is unclear.

To clarify the role of FDG-PET in the diagnosis of LMS, ESS and CS, FDG uptake was evaluated in patients with uterine sarcoma and LM. FDG uptake in patients with EC was evaluated as a reference. Serum LDH levels and CA-125 were also measured because high CA 125 levels occur in patients with uterine malignancies. The accuracy of FDG-PET

---

*Correspondence to:* Dr Naohiko Umesaki, <sup>3</sup>Present address: Department of Gynecology, Izumi Municipal Hospital, 4-10-10 Fuchu-cho, Izumi City, Osaka 594-007, Japan  
E-mail: umesaki@izumi-hp.com

**Key words:**  $^{18}\text{F}$ -fluorodeoxyglucose positron emission tomography, uterine sarcoma, leiomyosarcoma, lactate dehydrogenase, glucose transporter-1

combined with serum LDH was evaluated for the diagnosis LMS.

LMS is a rare disease, and uterine smooth muscle tumors of uncertain malignant potential (UMP) and bizarre LM (BLM), which are variants of LM (12), are also rare. Therefore, the number of such cases undergoing FDG-PET is small. The mortality associated with UMP and BLM is very low, though they can behave in a malignant fashion.

A correlation between glucose transporter-1 (GLUT-1) expression and FDG uptake has been reported in ovarian cancer (13) and pancreatic cancer (14), and GLUT-1 expression was therefore evaluated by immunohistochemistry. The potential role of FDG-PET in the differential diagnosis of LM, UMP, BLM and LMS is discussed.

## Patients and methods

**PET study.** The results of PET in three groups of patients were included. a) Patients who met more than one of the following criteria: i) Uterine tumor with unusual MRI findings (high intensity on T1-weighted and/or T2-weighted images), ii) rapidly enlarged tumor (enlargement of >2 times original volume within 1 year) and iii) serum LDH level  $\geq 229$  U/l. LM was identified on the basis of the pathological findings. This group was called the LM A group, and needed clinical differentiation from patients with LMS (15).

Even if the above criteria were not met, PET was performed at the patient's request. Patients in whom the pathological findings indicated LM were classified in the LM B group; none of these patients had LMS. b) The results of FDG-PET examinations in patients with clinically suspected uterine malignancies based on the results of Pap smear tests, endometrial curettage or MRI, were also included when uterine malignancies were revealed by pathological examination. c) The results of previously reported sarcoma cases (9) were also included in this study. There were 15 cases in the LM A group, nine in the LM B group, 19 cases of EC, four of LMS, five of CS and one case of ESS.

**Immunostaining of GLUT-1.** Immunostaining was performed in nine cases of LM (LM: 7 cases, UPM: 1 case, BLM: 2 cases) six cases of EC, 17 cases of sarcoma (CS: 7 cases, LMS: 7 cases, ESS: 3 cases) were performed. In some of these cases, FDG-PET was not performed.

**FDG-PET.** Radiolabeled FDG was produced at the cyclotron facility of the Wakayama PET Center. Whole-body PET using  $^{18}\text{F}$ -FDG was performed using a SET-3000B/l 3D-PET camera system (Shimadzu Co., Kyoto, Japan). The matrix size was 128x128, with a pixel size of 4x4 mm. After at least 5 h fasting, patients were intravenously administered FDG (2.6 MBq/kg body weight). Transmission and emission images were obtained simultaneously after 50 min (50-70 min after FDG injection). A region of interest (ROI) was placed over the most intense area of FDG accumulation. The PET images were quantitatively analyzed retrospectively using standard uptake values (SUVs), which were calculated using the following equation:

$$\text{SUV} = \frac{\text{tissue concentration (MBq/g)}}{\text{injection dose (MBq) / body weight (g)}}$$

**CT.** All patients underwent CT (Brilliance CT 40; Philips, Eindhoven, The Netherlands) examination of the abdomen and pelvis, except for the previously reported cases. CT scans were obtained with 2.0-mm thick axial planes in the upper portion of the abdomen and pelvis. The matrix size was 512x512, and the pixel size was 0.6x0.6 mm.

**Image fusion method.** We used a commercially available DICOM image fusion software program (PSP Co., Tokyo, Japan) to enable digital fusion of the images. The software automatically adjusted the pixel size. After the fusion area was manually selected on the transmission image according to the body shape, the fit image was registered on an image workstation according to a fusion algorithm based on minimizing the intensity difference. The emission image corresponding to the transmission image was then automatically displayed transparently over the CT image. Fine adjustments were performed manually when necessary.

**MRI.** MRI was performed using a 1.5-T imaging system (Intera Achieva 1.5T; Philips). Sagittal, axial and coronal T1-weighted images and T2-weighted fast spin echo images of the pelvis were acquired using a pelvic phased array coil.

**Serum LDH and CA-125 assays.** LDH converts pyruvate to lactate with the concomitant oxidation of NADH to NAD<sup>+</sup>. LDH is detected due to a decrease in absorbance at 340 nm resulting from the oxidation of NADH. An LDH assay kit (N-assay L LDH, Nitobo Medical Co., Tokyo, Japan) was used in this study. The normal limit of LDH is 229 U/l in our institution. CA-125 was assayed using an automated chemiluminescent enzyme immunoassay system (Lumipulse CA 125II, Fujirebio Diagnostic Inc., Tokyo, Japan).

**Histological examination.** Tissue sections were prepared from formalin-fixed and paraffin-embedded tissues of various uterine tumors obtained at surgery or biopsy. GLUT-1 was detected by immunohistochemistry using the labeled streptavidin-biotin (LSAB) procedure. Sections (3  $\mu\text{m}$ ) were cut from paraffin-embedded tissue blocks and deparaffinized. All sections were unmasked using the microwave method prior to immunohistochemistry using a citrate buffer, (pH 6.0) for 40 min. Endogenous peroxidase was neutralized with 0.3% hydrogen peroxidase for 30 min. The samples were then washed and incubated at room temperature for 1 h in a 1:50 dilution of polyclonal rabbit antihuman GLUT-1 antibody (Imgenex, CA, USA) raised against a 12-amino acid synthetic peptide corresponding to the carboxyl terminus of human GLUT-1. Parallel sections were incubated with healthy rabbit immunoglobulin G as a negative control. The samples were then washed, and biotinylated secondary antibody (Dako LSAB kit, Dako Cytomation, Inc., CA, USA) biotinylated anti-mouse, anti-rabbit, and anti-goat was applied to the slides for 45 min in a humidity chamber. The slides were again washed and incubated with streptavidin peroxidase for an additional 45 min and then submerged in a diaminobenzidine (DAB) bath for 5 min. Tissues were counterstained with hematoxylin. Staining intensity was used to categorize GLUT-1 immunoreactivity as follows: negative (grade 0), weak (grade 1), moderate (grade 2) and strong (grade 3).

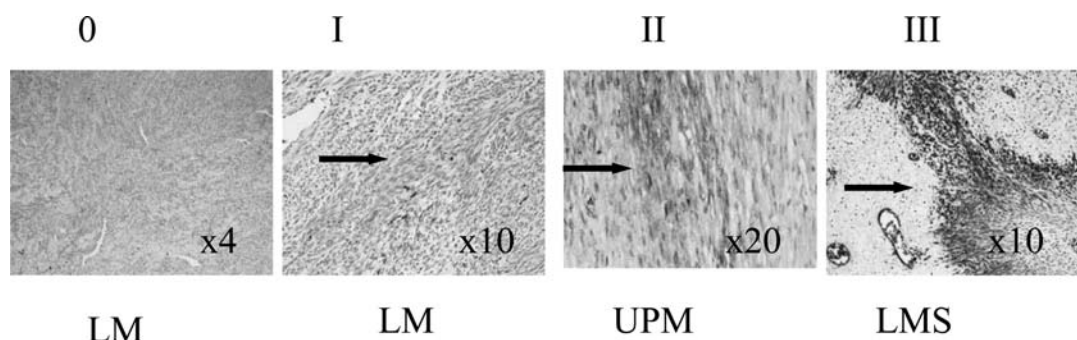


Figure 1. GLUT-1 staining intensity. Staining intensity was classified as grade 0 to grade 3. Arrows indicate GLUT-1 staining positive cells.

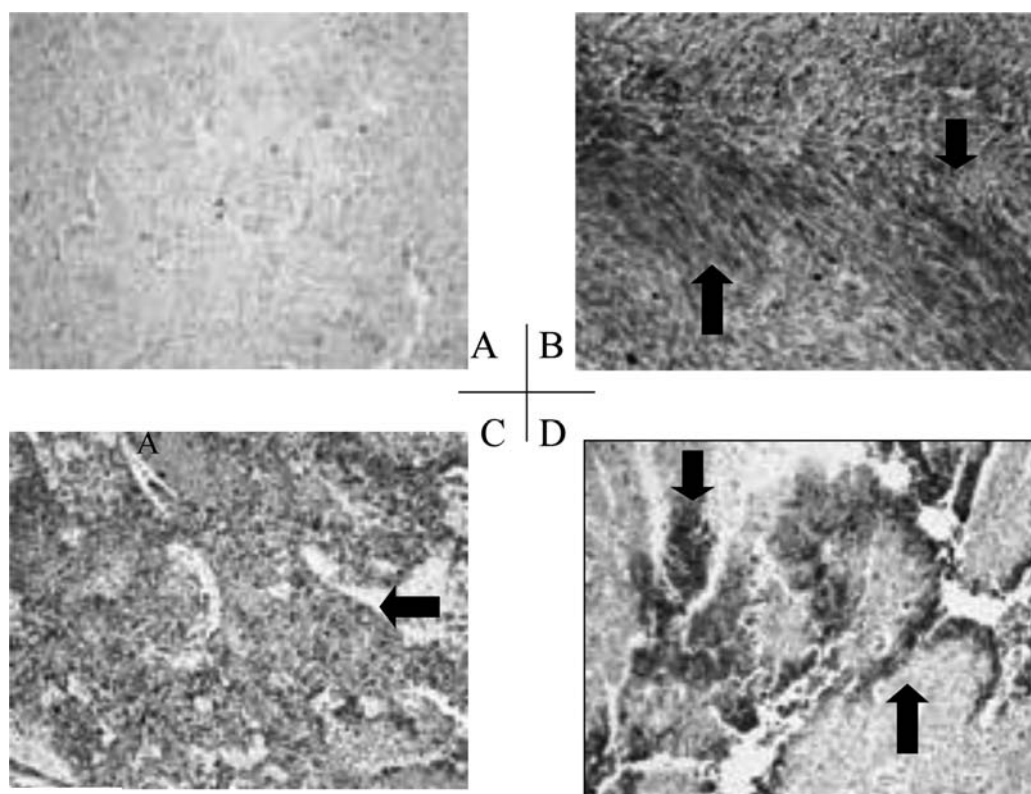


Figure 2. Expression of GLUT-1 in LMS (B, C, D) and LM (A). The GLUT-1 score for LMS was 9 and that for LM was 0. Arrows indicate GLUT-1 staining positive cells.

Strong staining was defined as the same staining intensity as red cells. Staining intermediate between strong and negative was categorized as moderate, while staining intermediate between moderate and negative was categorized as weak. The intensity grades are shown in Fig. 1. Proportional grades were categorized as follows: no stain (grade 0), <10% (grade 1), <20% (grade 2), and  $\geq 20$  (grade 3). The GLUT-1 expression score was calculated as:

$$\text{Intensity grade} \times \text{Proportional grade}$$

Staining was observed in LM and LMS cells. GLUT-1 expression in LMS and LM is shown in Fig. 2.

**Statistical analysis.** Data were analyzed using Stat View software (version 5) for Macintosh and  $p < 0.05$  was considered statistically significant. Unpaired t-tests were applied to assess

the significance of differences in SUV between two groups. Comparisons among three or more groups were analyzed using one-way factorial ANOVA and multiple comparison tests (Scheffe). Pearson's correlation coefficient was used to evaluate the relationships between GLUT-1 intensity and SUV. A conventional receiver operating characteristic (ROC) curve was used to determine the cut-off points that yielded the highest combined sensitivity and specificity for distinguishing LMS from LM.

## Results

Results are shown in box plots (Figs. 3-8 and 10-13).

**SUVs in LM.** The mean  $\pm$  SD of the SUVs in the LM A and LM B groups were  $2.75 \pm 0.61$  (range 1.60-3.99.) and  $2.35 \pm 0.38$  (range: 1.92-2.89), respectively. There was a tendency toward

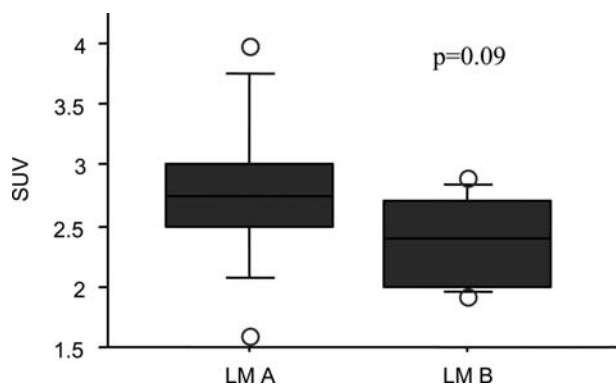


Figure 3. Comparison of SUVs between LM A and LM B.

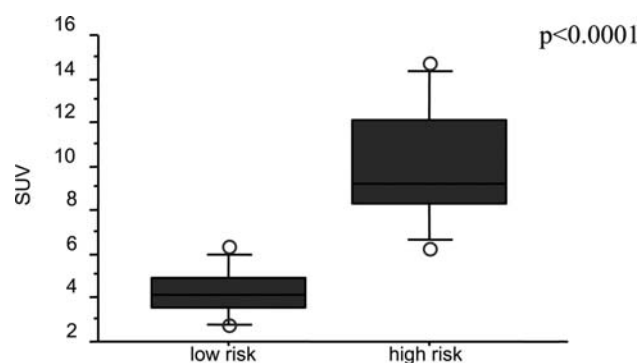


Figure 6. Comparison of SUVs between low-risk and high-risk EC groups.

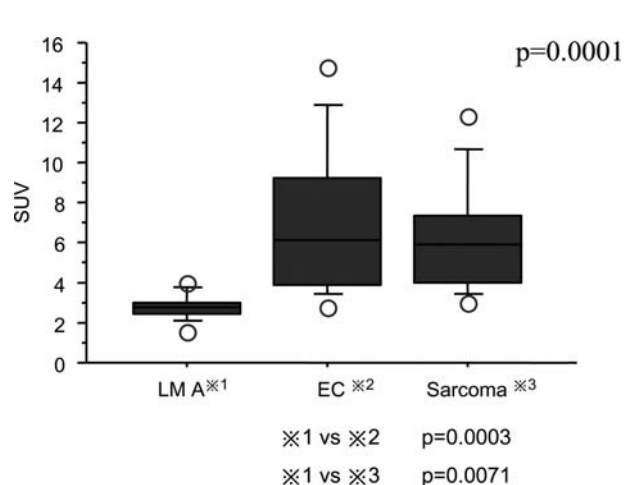


Figure 4. Comparison of SUVs among LM A, EC and sarcoma.

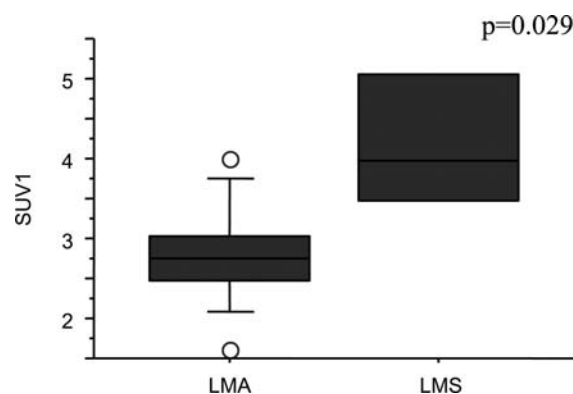


Figure 7. Comparison of SUVs between LM A and LMS.

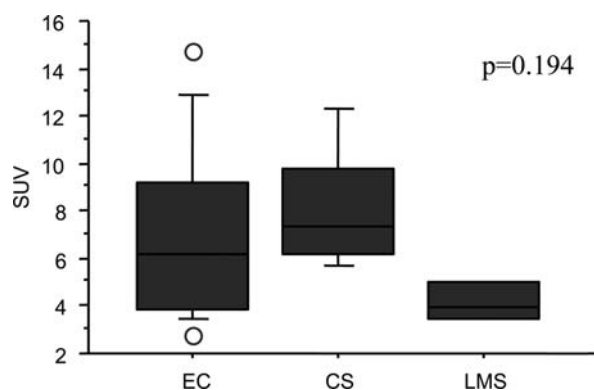


Figure 5. Comparison of SUVs among EC, CS, and LMS.

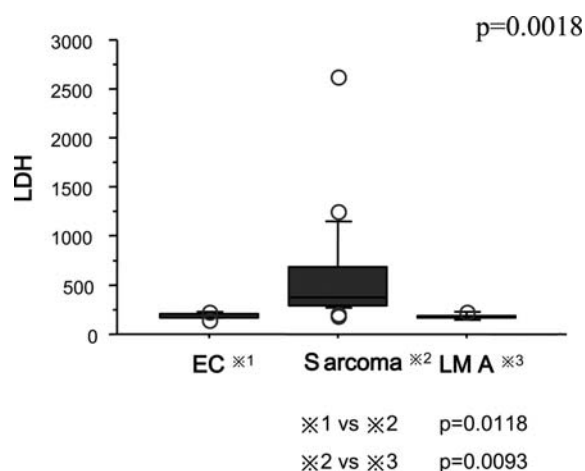


Figure 8. Comparison of LDH levels among EC, sarcoma and LM A.

a difference between the two groups, but this did not reach significance ( $p=0.09$ ) (Fig. 3).

**Comparison of SUVs among LM A, EC and sarcoma groups.** The mean  $\pm$  SD of the SUVs in the EC and sarcomas groups were  $7.12 \pm 0.60$  (range: 1.60-3.99) and  $6.31 \pm 2.74$  (range: 3.00-12.3), respectively. The difference among the three groups was significant ( $p=0.0001$ ). The differences between the LM A and EC groups ( $p=0.0003$ ) and between the LM A and sarcoma groups ( $p=0.0071$ ) were also significant (Fig. 4).

**Comparison of SUVs among EC, CS and LMS groups.** The mean  $\pm$  SD of the SUVs in the CS and LMS groups were  $8.12 \pm 2.65$  (range: 5.71-12.3) and  $4.26 \pm 1.31$  (range: 3.00-6.10), respectively. There were no differences among the EC, CS and LMS groups (Fig. 5).

**FDG-PET for EC.** We divided patients with EC into high- and low-risk groups on the basis of histological grade and depth of invasion. The high-risk group included tumors of grade III or depth C, and the low-risk group included the remainder



Table I. Comparison of accuracy of PET alone, serum LDH alone, and PET combined with serum LDH for diagnosis of LMS.

Diagnostic category	TP	TN	FP	FN	Sensitivity (%)	Specificity (%)	Accuracy (%)	PPV (%)	NPV (%)
PET	4	11	4	0	100	73	79	44	100
LDH	4	13	2	0	100	87	89	67	100
PET + LDH	4	15	0	0	100	100	100	100	100

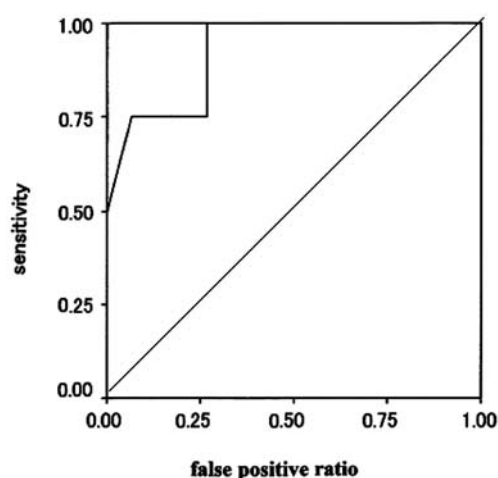


Figure 9. ROC.

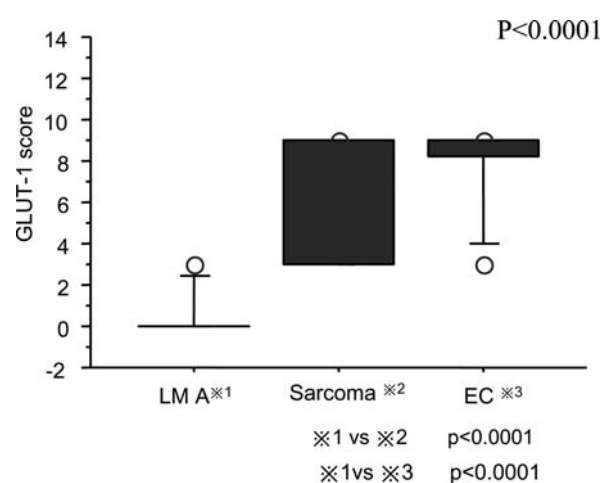


Figure 11. Comparison of GLUT-1 score among LM A, sarcoma and EC.

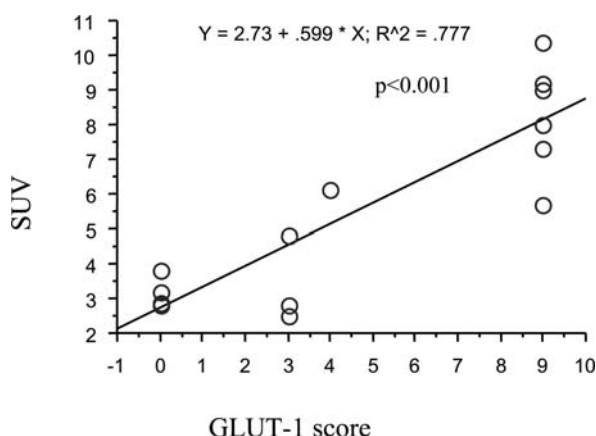


Figure 10. Relationship between SUV and GLUT-1 score in uterine tumors.

of the patients. There was a significant difference in SUVs between the low-risk and high-risk groups ( $p<0.0001$ ) (Fig. 6).

**Comparison of SUVs between LM A and LMS groups.** There was a significant difference in SUVs between the LM A and LMS groups ( $p=0.003$ ) (Fig. 7).

**Comparison of LDH levels among EC, sarcoma and LM A groups.** There were significant differences in LDH levels among the EC, sarcoma and LM A groups ( $p=0.0018$ ). The differences between the sarcoma and EC ( $p=0.0118$ ) and sarcoma and LM A ( $p=0.0023$ ) groups were also significant. However, there was no significant difference between the EC

and LM A groups (Fig. 8), or among the CS, LMS and ESS groups.

**Comparison of CA-125 among EC, sarcoma and LM A groups.** There was no significant difference in levels of CA-125 among the EC, sarcoma and LM A groups, or between the sarcoma and LM A groups.

**Estimation of SUV cut-off value between LMS and LM A.** A cut-off SUV value of 3 was determined, based on an ROC curve (Fig. 9).

**Comparison of accuracy of PET alone, serum LDH alone, and PET combined with serum LDH for diagnosis of LMS.** True positive (TP), true negative (TN), false positive (FP), false negative (FN), sensitivity (%), specificity (%), accuracy (%), positive predictive value (PPV) (%) and negative predictive value (NPV) (%) are shown for each diagnostic method (Table I). The accuracies of PET alone, serum LDH alone, and PET combined with serum LDH for diagnosis of LMS were 73, 87 and 100%, respectively (Table I).

**Relationship between SUV and GLUT-1 score in uterine tumors.** There was a strong correlation between SUV and GLUT-1 score in the uterine tumors examined ( $p<0.001$ ,  $r^2=0.777$ ) (Fig. 10).

**Comparison of GLUT-1 scores among LM, sarcoma and EC groups.** The mean  $\pm$  SD of the GLUT-1 scores for LM, CS, LMS, ESS and EC were  $0.43 \pm 1.13$  (range: 0.00-3.00),

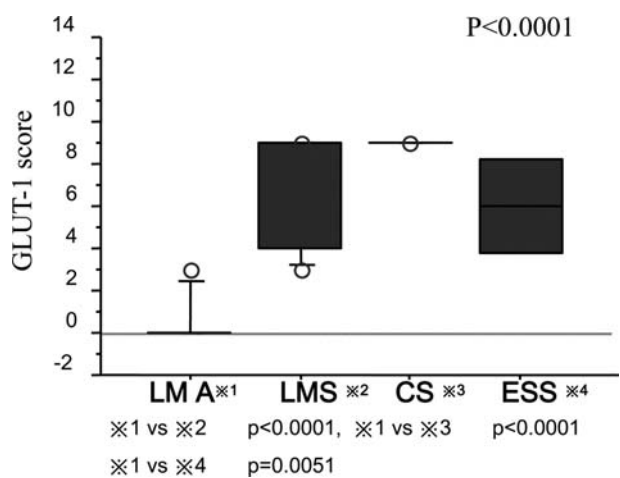


Figure 12. Comparison of GLUT-1 score among LM A, LMS, CS and ESS.

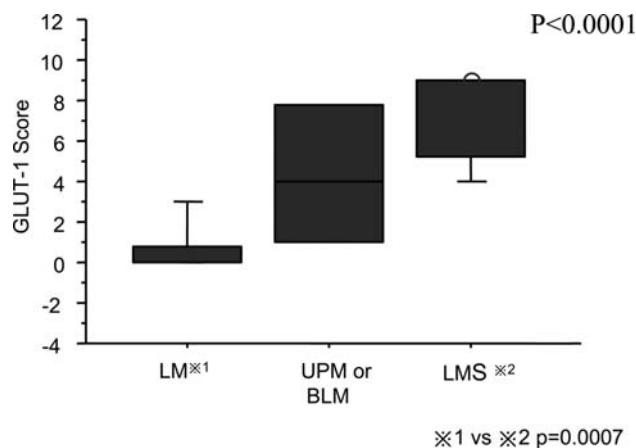


Figure 13. Comparison of GLUT-1 score among LM A, UPM or BLM and LMS.

9.00±0.00 (range: 9.00-9.00), 6.71±2.87 (range: 3.00-9.00), 6.00±3.00 (range: 3.00-9.00) and 9.00±0.00 (range: 9.00-9.00), respectively. The differences among the LM, sarcoma and EC groups ( $p<0.0001$ ) (Fig. 11), the LM A, LMS, CS and ESS groups ( $p<0.0001$ ), and between the LM A and LMS ( $p<0.0001$ ), LM A and CS ( $p<0.0001$ ), and LM A and ESS ( $p=0.0051$ ) groups were significant (Fig. 12).

*Comparison of GLUT-1 score among either LM, UPM or BLM and LMS groups.* There were significant differences in GLUT-1 scores among the three groups ( $p<0.0001$ ). There was also a significant difference between the LM and sarcoma groups ( $p=0.0007$ ), but no significant difference between the LM and UPM or BLM groups. However, high GLUT-1 expression was detected in one case of UPM (score 9) and one case of BLM (score 4) (Fig. 13).

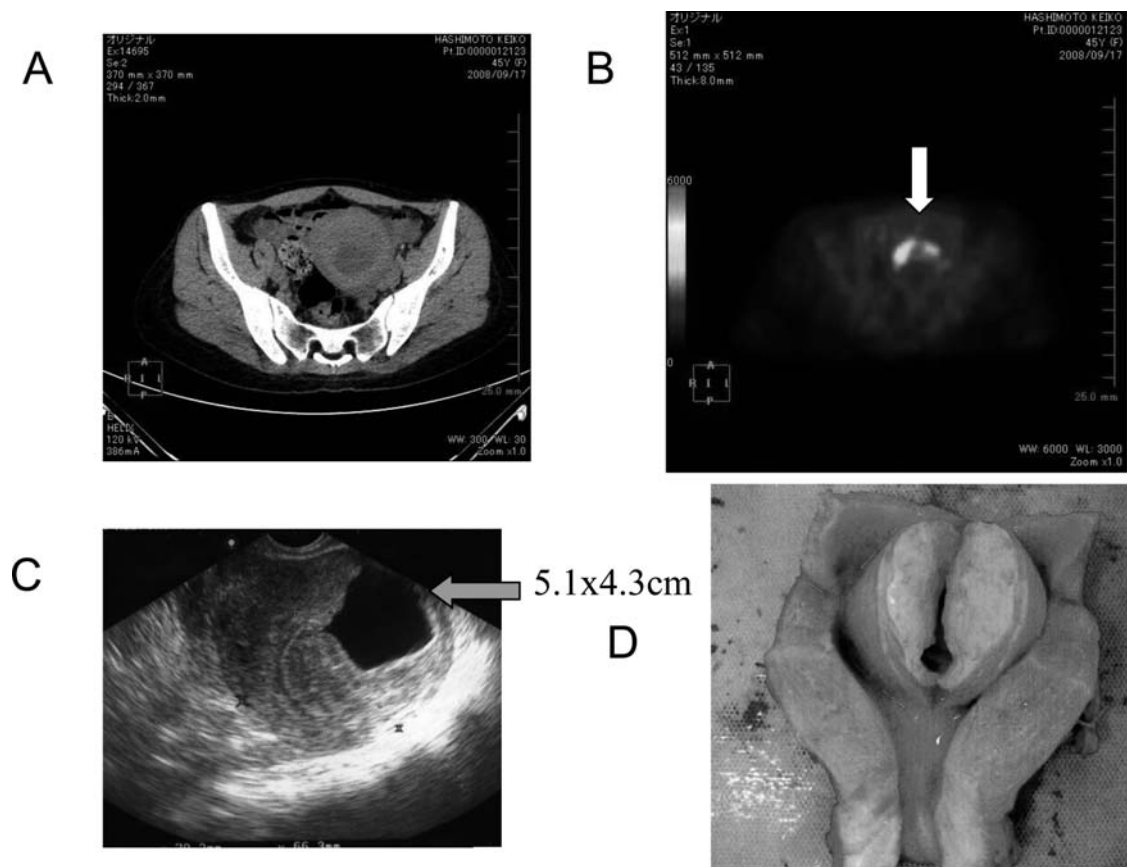


Figure 14. LM A case with an SUV of 3.99. (A) MRI, (B) PET-CT, (C) B-scope, (D) macro(adenomyoma). FDG uptake occurred around the cystic area.

## Discussion

Patients with LM were used as controls in this study and were divided into two groups: LM A patients who needed to be differentiated from LMS patients, and LM B patients who did not. The LM A group was identified by unusual MRI findings (high intensity on T1-weighted image), rapidly enlarging tumors, or high levels of LDH. Both groups were identified as LM by pathological examination of post-operative specimens. SUVs showed a tendency toward a difference between the LM A and LM B groups, but this difference was not significant ( $p=0.09$ ). The LM A group was therefore used as a control to differentiate from uterine sarcoma. EC patients were also included as a reference. LMS is a relatively rare tumor, and previously reported cases of LMS were therefore included in this study.

The SUVs for FDG in the EC and uterine sarcoma groups were significantly higher than in the LM group, suggesting that PET could be a useful diagnostic method for distinguishing uterine sarcomas and EC from LM. The high FDG SUV value for EC is less important, as EC can be easily diagnosed using other methods, such as Pap smear tests or by histological examination of endometrial tissue sampled during endometrial curettage. SUVs were significantly higher in the high-risk EC group than in the low-risk group, and PET could therefore be useful for identifying high-risk EC patients. Treatment strategies for EC include simple total hysterectomy with lymphadenectomy. In low-risk patients, lymphadenectomy may be limited to pelvic lymphadenectomy, but it may be extended to the paraaortic lymph nodes in high-risk patients. Preoperative determination of patients as high- or low-risk is therefore important.

There were no differences in FDG SUVs among EC, CS and LMS patients. However, there was a significant difference between the LM A and LMS groups, and an SUV cut-off value of 3 for differentiating between these groups was calculated using a ROC curve. The sensitivity, specificity and accuracy of this cut-off value for the diagnosis of LMS were evaluated and found to be 100, 73, and 79%, respectively. An accuracy of 79% is relatively low. We therefore evaluated the four cases of LM with SUVs  $>3.0$ : two cases with SUVs of 3.75 and 3.99 were adenomyomas with cystic formation in the myometrium. The case with an SUV of 3.99 is shown in Fig. 14. Two further cases with SUVs of 3.06 and 3.16 were cases of adenomyosis, in which GLUT-1 expression was noted in the glandular and stromal tissues. These results suggest that adenomyomas and adenomyosis were excluded by this SUV value. However, cases of adenomyomas with cystic areas can be easily diagnosed by MRI. If these cases were excluded, the diagnostic accuracy of LMS based on SUV increased to 88%.

High serum LDH levels have been reported in LMS. In this study, we found a significant difference in LDH levels between LM and LMS patients. We therefore evaluated the diagnostic accuracy of SUV combined with serum LDH levels for differentiating between LM and LMS. If both SUV and LDH were positive, the diagnostic accuracy for LMS was 100%. The combined use of imaging and measurement of serum LDH levels has already been reported (5). The previous study used MRI and the diagnostic accuracy for the

differential diagnosis of LM and LMS was 99.3%. In these studies, combined imaging and measurement of LDH were useful in differentiating between LMS and LM. Further studies are needed to compare the relative values of PET and MRI for the differential diagnosis of LMS and LM. However, the evaluation of MRI findings is subjective, while that of PET findings is objective, which suggests that PET could be preferable to MRI for the diagnosis of LMS.

FDG-PET can be used for diagnosing cancer because of the increased rate of glucose metabolism compared with benign disease, and overexpression of glucose transporters has been reported in several malignancies. Brown *et al* (16) reported a significant positive correlation between glucose transporter expression and FDG accumulation in viable cancer cells in syngeneic rat breast cancer. Evidence of a significant correlation between FDG accumulation and glucose transporter expression has also been found in human studies (14). There are five subtypes of glucose transporters. GLUT-1 plays a significant role in malignant glucose metabolism and may contribute to the increased uptake of FDG in PET imaging (14).

LMS is a rare tumor and the number of PET examinations performed was therefore small. GLUT-1 expression in LMS was examined to assess its correlation with high SUV values. LM includes UPM and BLM variants. The mortality associated with these tumors is very low, though they can sometimes behave in a malignant fashion. Immunohistochemical analysis of p16 expression in uterine smooth muscle tumors showed positive staining in 100% of LMS and UPM cases and 86.5% of BLM cases, compared with only 14% of LM cases. p53-immunostaining was positive in 91% of LMS cases, 60% of BLM cases, 50% of UPM cases and 0% of LM cases (17). These results suggest that UPM and BLM have intermediate characteristics between benign and malignant tumors. GLUT-1 scores were determined by staining intensity and proportion of stain with reference to the score of Allred *et al* (18). In our study, the SUV and GLUT-1 scores were well correlated. The GLUT-1 score for LMS was  $6.71 \pm 2.87$ , which was significantly higher than that for LM ( $0.43 \pm 1.13$ ). FDG-PET was only performed in one case of ESS, which showed an SUV of 4.0. The GLUT-1 score for the ESS group (3 cases) was  $6.00 \pm 3.0$ . Moderate staining scores were noted in some cases of UPM and BLM, and one case of BLM had a positive SUV value. Further studies are needed to clarify the efficacy of FDG-PET for the diagnosis of UPM and BLM.

In conclusion, although this study was limited by the small number of patients available for evaluation, the results suggest that FDG-PET could be useful for the differential diagnosis of uterine sarcomas. FDG-PET combined with serum LDH levels was more accurate than either method alone for the diagnosis of LMS. GLUT-1 expression analysis confirmed the usefulness of FDG-PET for the diagnosis of LMS.

## Acknowledgements

We thank Dr M. Terada (Wakayama PET Center) for evaluation of PET findings, and Dr Y. Nakamura (Department of Clinical Laboratory Medicine, Wakayama Medical University) for evaluation of pathological specimens.

## References

1. Adamson GD: Treatment of uterine fibroids: current findings with gonadotropin-releasing hormone agonists. *Am J Obstet Gynecol* 166: 746-751, 1992.
2. Hurst BS, Stackhouse DJ, Matthews ML and Marshburn PB: Uterine artery embolization for symptomatic uterine myoma. *Fertil Steril* 74: 855-869, 2000.
3. Okizuka H, Sugimura K, Takemori M, Obayashi C, Kitao M and Ishida T: MR detection of degenerating uterine leiomyomas. *J Comput Assist Tomogr* 17: 760-766, 1993.
4. Seki K, Hoshihara T and Nagata I: Leiomyosarcoma of the uterus: ultrasonography and serum lactate dehydrogenase level. *Gynecol Obstet Invest* 33: 114-118, 1992.
5. Goto A, Takeuchi S, Sugimura K and Maruo T: Usefulness of Gd-DTPA contrast-enhanced dynamic MRI and serum determination of LDH and its isozymes in the differential diagnosis of leiomyosarcoma from degenerated leiomyoma of the uterus. *Int J Gynecol Cancer* 12: 354-361, 2002.
6. Rohren PG, Turkington TG and Coleman RE: Clinical applications of PET in oncology. *Radiology* 231: 305-332, 2004.
7. Umesaki N, Tanaka T, Miyama M, Ogita S and Ochi H: Combined diagnostic imaging of uterine sarcoma: A case report. *Int J Gynecol Cancer* 10: 425-428, 2000.
8. Umesaki N, Tanaka T, Miyama M, *et al*: Positron emission tomography with 18F-fluoro-deoxyglucose in the diagnosis of uterine leiomyosarcoma: A case report. *Clin Imaging* 25: 203-205, 2001.
9. Umesaki N, Tanaka T, Miyama M, *et al*: Positron emission tomography with 18F-fluorodeoxyglucose of uterine sarcoma: a comparison with magnetic resonance imaging and power doppler imaging. *Gynecol Oncol* 80: 372-377, 2001.
10. Ak L, Ozalp S, Yalcin OT, *et al*: Uptake of 2-[18F]fluoro-2-deoxy-D-glucose in uterine leiomyoma; imaging of four patients by coincidence positron emission tomography. *Clin Nucl Med* 259: 941-945, 2004.
11. Shida M, Murakami M, Tsukada Y, *et al*: F-18 fluoro-deoxyglucose uptake in leiomyomatous uterus. *Int J Gynecol Cancer* 17: 285-290, 2006.
12. Hendrickson MR and Kempson RL: Pure mesenchymal neoplasms of the uterine corpus. In: Haines and Taylor *Obstetrical and Gynecological Pathology*. Fox H and Wells M (eds). 4th edition, Churchill Livingstone, New York, pp519-586, 1995.
13. Higashi T, Tamaki N, Honda T, *et al*: Expression of glucose transporters in human pancreatic tumors compared with increased FDG accumulation in PET study. *J Nucl Med* 38: 1337-1344, 1997.
14. Kurokawa T, Yoshida Y, Kawahara K, *et al*: Expression of GLUT-1 glucose transporter, cellular proliferation activity and grade of tumor correlate with [F-18]-fluorodeoxyglucose uptake by positron emission tomography in epithelial tumors of the ovary. *Int J Cancer* 109: 926-932, 2004.
15. Kawamura N, Ichimura T, Ito F, *et al*: Transcervical needle biopsy for the differential diagnosis between uterine sarcoma and leiomyoma. *Cancer* 94: 1713-1720, 2001.
16. Brown RS, Leung JY, Fisher SJ, Frey KA, Ethier SP and Wahl RL: Intratumoral distribution of tritiated FDG in breast carcinoma: correlation between Glut-1 expression and FDG uptake. *J Nucl Med* 37: 1042-1047, 1996.
17. Chen L and Yang B: Immunohistochemical analysis of p16, p53, and KI-67 expression in uterine smooth muscle tumors. *Int J Gynecol Pathol* 27: 326-332, 2008.
18. Allred DC, Harvey JM, Berardo M and Clark GM: Prognostic and predictive factors in breast cancer by immunohistochemical analysis. *Mod Pathol* 2: 155-168, 1998.